Complex anisotropy ratio of third harmonic generation in semiconductor using terahertz free electron laser

THANH NHAT KHOA PHAN,[1] YOU WEI WANG,[1] TOMOKI SHIMIZU,[1] KOSAKU KATO,[1] VERDAD C. AGULTO,[1] GORO ISOYAMA,[2] SHINSUKE FUJIOKA,[1] AND MAKOTO NAKAJIMA[1,*]

[1]*Institute of Laser Engineering, Osaka University, 2-6 Yamadaoka, Suita, Osaka 565-0871, Japan*
[2]*SANKEN (Institute of Scientific and Industrial Research), Osaka University, 8-1 Mihogaoka, Ibaraki, Osaka 567-0047, Japan*
*nakajima.makoto.ile@osaka-u.ac.jp

Received XX Month XXXX; revised XX Month, XXXX; accepted XX Month XXXX; posted XX Month XXXX (Doc. ID XXXXX); published XX Month XXXX

The nonlinear susceptibility in the terahertz region is expected to have a non-negligible imaginary part originating from the momentum-dependent scattering time of free carriers, but it has been scarcely reported. By utilizing an intense 4-THz beam from a terahertz free electron laser, we investigated the azimuth angle dependence of the third harmonic generation (THG) from semiconductors. The observed angular anisotropy of THG revealed the contribution of the imaginary part of the nonlinear susceptibility originating from the momentum-scattering time relation in addition to its real part originating from the band nonparabolicity. The results provide a deeper understanding of nonlinear optics in the terahertz region.

In recent years, the study of physics phenomena in the terahertz (THz) frequency range has experienced immense development, both in fundamental researches and practical application [1–15]. Specifically, the research of harmonic generation (HG) in terahertz (THz) and far-infrared (FIR) region has picked up its pace recently with the advent of strong THz excitation source, such as femtosecond (fs) laser-based sources and free electron laser (FEL) [16–19]. The merits of FEL include strong pulse energy (tens of mJ), short pulse duration, narrow bandwidth, tunable wavelength, and high coherence. Since the advent of such strong THz sources, the study of HG in FIR-THz has made significant progresses with high nonlinear susceptibility χ and harmonic conversion efficiency [20–25].

The HG in the THz region is mainly ascribed to the nonlinear response of free carriers to the electric field [20–25]. The predominant and frequently discussed cause of this nonlinear response is the nonparabolicity of the conduction band [26], which makes the effective mass of carriers m^* in a crystal dependent on their momentum p. On the other hand, the scattering time τ of carriers also depends on the momentum p, and this can also be the origin of the nonlinear response [27–29]. Interestingly, while the value of the nonlinear susceptibility originating from nonparabolicity, χ_{NP}, tends to be real, the one originating from the momentum-dependent scattering time, χ_{SC}, tends to be nearly pure imaginary [29]. Note that the imaginary part of the nonlinear susceptibility is zero when the nonlinear medium is lossless [30], which is often a good approximation for HG in transparent nonlinear optical crystals utilized in the visible range. However, since the HG in the THz region mainly stems from free carriers, it is inevitably affected by the energy loss due to the carrier scattering. In addition, due to the intense THz field employed as a fundamental of HG, the scattering events and the resulting energy loss will be further increased by nonperturbative processes such as impact ionization, tunneling ionization and phonon emission [31]. Therefore, the effect of the carrier scattering and the resulting imaginary part of the nonlinear susceptibility is in general not negligible in THz HG.

The imaginary part or complex phase of the nonlinear susceptibility cannot be obtained just by measuring the third harmonic generation (THG) intensity at one configuration. However, the complex phase is reflected in the dependence of HG efficiency on the polarization states of pumping field with respect to the crystal orientation. Using this effect, the complex phase difference as well as the magnitude ratio between the susceptibility tensor components has been evaluated for the THG in the visible and near-infrared region [32,33]. While the real part of the third-order susceptibility has been widely studied across various frequency regions, research on the imaginary part has been limited to the visible and near-infrared regions (frequency above 150 THz [32–34]), driven by the availability of intense light sources and vast practical applications [34,35]. There have been no reports in the THz or FIR region on the THG susceptibility including its complex phase or imaginary part, in spite of its importance in this frequency range.

In this paper, we investigated the THG of 4 THz output from FEL in semiconductors to evaluate the complex phase difference between the susceptibility tensor components. The dependence of THG intensity on azimuthal angle ϕ between the crystal axis and FEL output polarization was analyzed for indium arsenide (InAs), indium antimonide (InSb), and silicon (Si) samples. We found that the complex phase difference is far from zero for all the samples,

showing that the susceptibility contains non-negligible imaginary part. Our results revealed the importance of momentum-dependent scattering time in addition to the nonparabolicity for THG in the THz and FIR region.

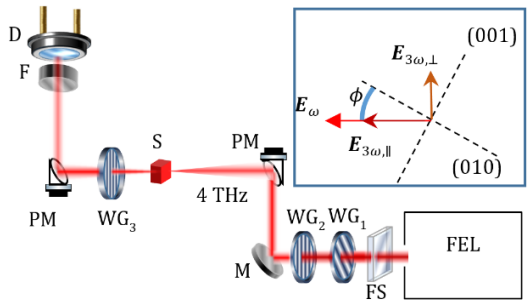

Fig. 1. Setup of the experiment. FS: fused silica; M: mirror; PM: parabolic mirror; WG: wire grid; F: CsBr filter; D: detector. Inset: orientation of the electric vectors of pump and THG beam, viewing along the direction normal to the sample surface. E_ω: electric field of the pumping beam. $E_{3\omega,\parallel}$ and $E_{3\omega,\perp}$: orthogonal components of the THG electric field with the polarization parallel and perpendicular to that of the pumping beam, respectively.

Fig. 1 shows the experiment setup. The FEL at the Research Laboratory for Quantum Beam Science, SANKEN (Institute of Scientific and Industrial Research), Osaka University [19,36,37] was used to excite the samples. The FEL emits 5 macro pulses per second, each contains ~110 micro pulses spacing 37 ns from each other. The output frequency was tuned to 4 THz (wavelength 75 μm). Intrinsic harmonics at 8 and 12 THz contained in the output [38] are filtered out by a 0.5 mm thick fused silica (FS) plate. Two wire-grid polarizers WG_1 and WG_2 were used to control the pumping beam intensity and polarization. The direction of the WG_2 was fixed so that the pump beam polarization became horizontal. The FEL beam was focused onto the sample surface, on which the spot size diameter and the macropulse energy density were 1.4 mm and ~0.1 J/cm^2, respectively. The samples were held on a motorized stage and rotated around the axis normal to their cut surface to change the angle ϕ (the azimuthal angle) between the crystal (010) axis and the polarization of the pumping beam (Inset of Fig. 1). And then, by switching the direction of the wire-grid polarizer WG_3, we selectively measured the intensity of the two orthogonal components of the THG electric field with the polarization parallel ($E_{3\omega,\parallel}$) and perpendicular ($E_{3\omega,\perp}$) to that of the pumping beam E_ω (see the inset of Fig. 1). A DLaTGS (JASCO Corp.) detector was used to measure the signal intensity. A 20 mm long CsBr crystal (F) was set before the detector to reject the residual 4-THz pumping beam. The measurement setup was purged by dried air to suppress the water vapor absorption. The measurements were performed at room temperature. We have confirmed that the second harmonic was not generated as discussed in our previous work [25] because of the absence of broken inversion symmetry necessary for the even-order harmonics [39].

The properties of the samples investigated in this work are summarized in Table 1. The InAs and InSb were n-type semiconductor while Si was boron-doped and p-type semiconductor. All the samples had a (100) surface. The carrier density, mobility, and the scattering rate were evaluated from the results of the THz time domain spectroscopy [13,25]. According to previous research [28,29], the nonlinear susceptibility originating from the nonparabolicity (i.e. χ_{NP}) can be regarded as a pure real number, while the one originating from the momentum-dependent scattering time (i.e. χ_{SC}) can be regarded as a pure imaginary number as long as the condition $(3\omega\tau)^{-1} \ll 1$ holds, i.e. when the scattering rate (inverse of the scattering time, $1/\tau$) is much lower than the generated frequency 3ω, which is 2π×12 THz in our case. This holds true for all the samples we investigated in this study.

Table 1. Characteristics of the samples used in this study at room temperature.

Sample	Surface	Thickness (μm)	Carrier density (cm^{-3})	Mobility (cm^{2}V^{-1}s^{-1})	Scattering rate 1/τ(THz)
InAs	(100)	470	1.4×10^{16}	1.8×10^{4}	4.2
InSb	(100)	430	1.2×10^{16}	6.2×10^{4}	2.0
Si	(100)	523	8.6×10^{14}	8.6×10^{2}	5.5

For (100)-cut samples with a cubic symmetry studied in the present work, the intensity dependence of the THG electric field component $I_{||} \propto |E_{3\omega,||}|^2$ and $I_\perp \propto |E_{3\omega,\perp}|^2$ on the azimuth angle ϕ can be expressed by only 2 independent elements of the susceptibility tensor χ_{xxxx} and χ_{xxyy} (abbreviated as χ_1 and χ_2, respectively) [30,40]:

$$I_\parallel \propto I_\omega^3 \left[(|A|^2 + |B|^2/2) + 2\mathrm{Re}(AB^*)\cos 4\phi + (|B|^2/2)\cos 8\phi\right] \quad (1)$$

$$I_\perp \propto I_\omega^3 |B|^2 (1 - \cos 8\phi), \quad (2)$$

where $A = 3(\chi_1 + \chi_2)$, $B = \chi_1 - 3\chi_2$, and I_ω is the intensity of the fundamental. By measuring the dependence of THG intensity $I_\perp$ and $I_\parallel$ on ϕ, one can extract the ratio between the two susceptibility tensor elements χ_{R} including its phase θ_{R} defined as:

$$\chi_{\mathrm{R}} = |\chi_{\mathrm{R}}| e^{i\theta_{\mathrm{R}}} = \chi_2/\chi_1 = \frac{A - 3B}{3A + 3B}. \quad (3)$$

The ratio χ_{R} is related with the normalized anisotropy σ appearing in [32,40] by $\sigma = B/\chi_1 = 1 - 3\chi_{\mathrm{R}}$. Note that there is an uncertainty about the sign of θ_R [33], and the value we obtained and show here is the magnitude of θ_R.

Fig. 2 shows the azimuth angle dependence of the THG intensity generated from the InAs(100) sample. The $I_\parallel$ [Fig. 2(a)] was modulated mainly with angular cycle 90°, corresponding to the $\cos 4\phi$ term in Eq. (1). However, the dips around 45° and 135° were much flatter than the peak around 90°, and had a small local maximum around each center. This deviation from the $\cos 4\phi$-like shape is considered to reflect the $\cos 8\phi$ term in Eq.(1). The $I_\perp$ [Fig. 2(b)] had an oscillation with angular cycle 45° in agreement with the $\cos 8\phi$ term in Eq.(2). To evaluate the value of χ_{R}, we fit these results by using Eqs. (1) and (2) as shown by solid curves in Fig. 2. From the fit, the absolute value and complex phase of χ_{R} was estimated to be $|\chi_{\mathrm{R}}| = 0.38 \pm 0.02$ and $\theta_{\mathrm{R}} = 85° \pm 3°$, respectively. Note that the obtained complex phase θ_{R} is far from zero and thus the imaginary part of the χ_{R} is considerably large. This result means that at least one of the nonlinear susceptibility tensor components χ_1 and χ_2 has a complex value.

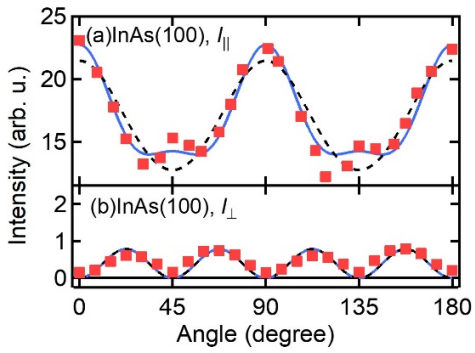

Fig. 2. Intensities of the THG component from the (100)-cut InAs polarized parallel (a) and perpendicular (b) to the polarization of the fundamental. Markers: measured intensities. Solid curves: fit results using Eqs. (1) and (2). Dashed curves: the same but θ_R is fixed to zero.

To confirm the importance of the complex phase, we also show by the dashed curves in Fig. 2(a) the fit with θ_R fixed to zero and $|\chi_R|$ found to be 0.18 ± 0.01. It does not reproduce the characteristic of $I_{\parallel}$ that the dips around 45° and 135° are wider than the peak around 90°. Allowing the complex value of χ_1 and χ_2 makes it possible to make the coefficient $2\mathrm{Re}(AB^*)$ of the $\cos 4\phi$ term in Eq. (1) small while keeping the constant term and $\cos 8\phi$ term large, which much improves the fit to the experimental result. Therefore, the observed vertically asymmetric dependence of $I_{\parallel}$ on the azimuth angle in Fig. 2(a) shows the considerable effect of the imaginary part in the nonlinear susceptibility.

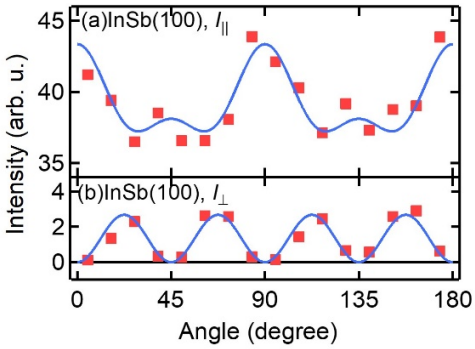

Fig. 3. Intensities of the THG component from the (100)-cut InSb, polarized parallel (a) and perpendicular (b) to the polarization of the fundamental. Markers: measured intensities. Solid curves: fit results using Eqs. (1) and (2)

Figs 3(a) and (b) show the azimuth angle dependence of $I_{\parallel}$ and $I_{\perp}$ for the InSb (100) sample, respectively. The maximum of the THG intensity $I_{\parallel}$ for this InSb is around twice as high as that for the InAs shown in Fig 2(a). Since the thickness and carrier density are similar between the two samples (Table 1), the higher THG efficiency of the InSb than the InAs is considered to mainly come from its larger nonparabolicity: InSb has smaller band gap and effective mass (0.175 eV [41] and 0.015 m_0 [42]) than InAs (0.36 eV [43] and $0.023m_0$ [44]), which provides the larger χ_{NP} than that of InAs [25,28]. The intensity of the THG from InSb again showed remarkable azimuth angle dependence with vertical asymmetry. Note that the band of InSb is almost spherical (except for high doping case [45]), which means $\chi_{2,NP} = 1/3\,\chi_{1,NP}$ [29]. Then if only the nonparabolicity contributed to THG, the nonlinear susceptibility would satisfy $\chi_R = 1/3$ [29] and thus $\sigma = 0$ and $B = 0$, according to Eq. (3). As a result, $I_{\parallel}$ would show no azimuth angle dependence and $I_{\perp}$ would vanish, according to Eqs. (1) and (2). Conversely, the observed clear azimuth angle dependence indicates the non-negligible contribution of the susceptibility χ_{SC} originating from momentum-dependent scattering time to the THG process, because $\chi_{2,SC} = 1/2\,\chi_{1,SC}$ [29]. We fit the experimental data by using Eqs. (1) and (2) and the fit curves are shown by the solid curves in Fig. 3. From this fit, the absolute value and complex phase of χ_R was estimated to be $|\chi_R| = 0.38 \pm 0.02$ and $\theta_R = 58° \pm 4°$, respectively. The complex phase θ_R for the InSb is smaller than that of the InAs. Though it is difficult to quantitatively explain this difference in θ_R, its possible origin is inferred as follows: as described above, InSb has a larger χ_{NP} than InAs due to its greater nonparabolicity. On the other hand, the scattering rate $1/\tau$ of the InSb sample is ~2 times lower than in the InAs (Table 1), which will result in smaller χ_{SC} [28]. Therefore, the contribution of the imaginary χ_{SC} to the total nonlinear susceptibility is less prominent for the InSb than the InAs, which can lead to a smaller complex phase θ_R.

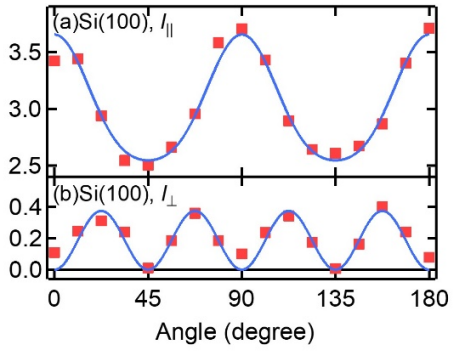

Fig. 4. Intensities of the THG component from the (100)-cut Si, polarized parallel (a) and perpendicular (b) to the polarization of the fundamental. Markers: measured intensities. Solid curves: fit results using Eqs. (1) and (2).

Both the InSb and InAs samples we discussed so far are n-type semiconductors. As an example of a p-type semiconductor, we measured a boron-doped Si sample and the results are shown in Fig. 4. The maximum of the THG intensity [Fig. 4(a)] is about 1/6 of the THG from InAs [Fig. 2(a)]. This low THG efficiency can be attributed to a small χ_{NP}, which is due to lower free carrier density (Table 1) combined with the smaller nonparabolicity expected from the larger band gap (1.1 eV [46]) and heavy effective masses ($0.16m_0$ for light hole and $0.49m_0$ for heavy hole [47]). The azimuth angle dependence of $I_{\parallel}$ [Fig. 4(a)] again has dips around 45° and 135° flatter than the peak around 90°, albeit no local maxima. We fit the experimental data by using Eqs. (1) and (2), and the fit curves are shown by the solid curves in Fig. 4. From this fit, the absolute value and complex phase of χ_R was estimated to be $|\chi_R| = 0.29 \pm 0.02$ and $\theta_R = 53° \pm 7°$, respectively. The complex phase θ_R was again far from zero, which indicates the

existence of the imaginary part in the THG susceptibility. Note that the azimuth angle dependence in THG intensity is readily expected for Si because its energy band is nonspherical [48], which inherently invalidates the relation $\chi_{2,\mathrm{NP}} = 1/3\,\chi_{1,\mathrm{NP}}$ [29] and causes $\sigma \neq 0$. However, the existence of the imaginary part in χ_{R} cannot be explained solely by the band nonparabolicity but suggests a non-negligible contribution of χ_{SC} due to a high scattering rate (Table 1).

The results shown above reveal that the nonlinear susceptibility of the THz-THG generally contains non-negligible imaginary part, which is ascribed to the momentum-dependent scattering time τ of carriers. The dependence of τ or scattering rate $1/\tau$ on the carrier momentum p is known for various carrier scattering mechanisms such as acoustic phonon, polar optical phonon and ionized impurity scattering [28,49,50]. In addition to this dependence commonly observed under weak electric field, nonlinear phenomena caused by the intense pumping field, such as impact ionization and phonon emission [51,52] would increase the phonon and electron/hole densities and impose additional dependence of $1/\tau$ on p. For now, the major origin of the momentum-dependent scattering time suggested from our measurement is yet to be elucidated. Though studies on THG from semiconductors in THz region are limited compared to those in shorter wavelength region, we hope that our study stimulates further investigations on THz-THG to facilitate the unveiling of its mechanism in more detail.

In summary, we reported the azimuthal angle dependence of the THG from InAs, InSb, and Si in the THz region for the first time. The strongest THG signal is from InSb and can be ascribed to its larger band-nonparabolicity, which contributes to the real part of the nonlinear susceptibility, compared to those of InAs and Si. However, the extracted anisotropy ratios $\chi_{\mathrm{R}} = \chi_2/\chi_1$ were found to be complex values, the reason of which is proposed to be the non-negligible contribution of momentum-dependence of scattering time to the imaginary part of the nonlinear susceptibility, in addition to the band-nonparabolicity. This study paves the way for better understanding of the nonlinear optical phenomena in semiconductors in the THz region.

Funding. Japan Society for the Promotion of Science KAKENHI (JP20H02206, JP23K17748, JP24H00317, JP24H02232).

Acknowledgment. We thank K. Furukawa and Y. Fukui for FEL operation. This work was performed by using the THz-FEL based on L-band Electron Linac at Research Laboratory for Quantum Beam Science, Institute of Scientific and Industrial Research, Osaka University.

Disclosures. The authors declare no conflicts of interest.

Data availability. Data underlying the results presented in this paper are not publicly available at this time but may be obtained from the authors upon reasonable request.

References

1. K. Makino, K. Kato, K. Takano, et al., Sci. Rep. **8**, 2914 (2018).
2. T. Kurihara, K. Hirota, H. Qiu, et al., Sci. Rep. **10**, 7231 (2020).
3. N. Yoshikawa, T. Tamaya, and K. Tanaka, Science (80-.). **356**, 736 (2017).
4. R. Matsunaga, N. Tsuji, H. Fujita, et al., Science (80-.). **345**, 1145 (2014).
5. A. Iba, C. W. Domier, M. Ikeda, et al., Opt. Lett. **46**, 4912 (2021).
6. M. A. Weiss, A. Herbst, J. Schlegel, et al., Nat. Commun. **14**, 7651 (2023).
7. J. Wang, W. Cai, W. Lu, et al., Nature DOI:10.1038/s41586 (2024).
8. Y. W. Wang, S. Segawa, T. Shimizu, et al., Appl. Phys. A Mater. Sci. Process. **128**, 836 (2022).
9. G. Fitzky, M. Nakajima, Y. Koike, et al., Phys. Rev. Lett. **127**, 107401 (2021).
10. D. Li, Y. Wang, M. Nakajima, et al., Appl. Phys. Lett. **110**, 151108 (2017).
11. D. Li, M. Nakajima, M. Tani, et al., Sci. Rep. **9**, 6804 (2019).
12. V. C. Agulto, T. Iwamoto, H. Kitahara, et al., Sci. Rep. **11**, 18129 (2021).
13. V. C. Agulto, K. Toya, T. N. K. Phan, et al., Appl. Phys. Lett. **118**, 42101 (2021).
14. M. Ota, K. Kan, S. Komada, et al., Nat. Phys. **18**, 1436 (2022).
15. M. Nagai, S. Aono, M. Ashida, et al., New J. Phys. **19**, 053017 (2017).
16. G. Ramian, Nucl. Instruments Methods Phys. Res. Sect. A Accel. Spectrometers, Detect. Assoc. Equip. **318**, 225 (1992).
17. D. Oepts, A. F. G. van der Meer, and P. W. van Amersfoort, Infrared Phys. Technol. **36**, 297 (1995).
18. Y. U. Jeong, B. C. Lee, S. K. Kim, et al., Nucl. Instruments Methods Phys. Res. Sect. A Accel. Spectrometers, Detect. Assoc. Equip. **475**, 47 (2001).
19. K. Kawase, R. Kato, A. Irizawa, et al., Nucl. Instruments Methods Phys. Res. Sect. A Accel. Spectrometers, Detect. Assoc. Equip. **726**, 96 (2013).
20. M. R. Siegrist, F. Keilmann, C. Nieswand, et al., Infrared Phys. Technol. **36**, 407 (1995).
21. K. J. Tielrooij, A. Principi, D. S. Reig, et al., Light Sci. Appl. **11**, 315 (2022).
22. H. A. Hafez, S. Kovalev, J. C. Deinert, et al., Nature **561**, 507 (2018).
23. T. A. Uaman Svetikova, T. V. A. G. de Oliveira, A. Pashkin, et al., ACS Photonics **10**, 3708 (2023).
24. F. Meng, M. D. Thomson, Q. Ul-Islam, et al., Phys. Rev. B **102**, 075205 (2020).
25. T. N. K. Phan, T. Shimizu, Y. W. Wang, et al., Opt. Lett. **49**, 1073 (2024).
26. P. A. Wolff and G. A. Pearson, Phys. Rev. Lett. **17**, 1015 (1966).
27. P. Kaw, Phys. Rev. Lett. **21**, 539 (1968).
28. C. C. Wang and N. W. Ressler, Phys. Rev. **188**, 1291 (1969).
29. K. C. Rustagi and S. S. Jha, Phys. Lett. A **30**, 518 (1969).
30. R. W. Boyd, "Nonlinear Optics," Third Ed. (Academic Press, 2008).
31. F. Meng, F. Walla, S. Kovalev, et al., Phys. Rev. Res. **5**, 043141 (2023).
32. W. K. Burns and N. Bloembergen, Phys. Rev. B **4**, 3437 (1971).
33. D. J. Moss, H. M. van Driel, and J. E. Sipe, Opt. Lett. **14**, 57 (1989).
34. P. A. Shaw, E. Forsyth, F. Haseeb, et al., Front. Chem. **10**, 921354 (2022).
35. K. D. Belfield, S. Yao, and M. V. Bondar, Adv. Polym. Sci. **213**, 97 (2008).
36. K. Kawase, M. Nagai, K. Furukawa, et al., Nucl. Instruments Methods Phys. Res. Sect. A Accel. Spectrometers, Detect. Assoc. Equip. **960**, 163582 (2020).
37. G. Isoyama, JAS4QoL **6**, 2 (2020).
38. R. Kato, R. A. V Kumar, M. Kuwahara, et al., Nucl. Instruments Methods Phys. Res. Sect. A Accel. Spectrometers, Detect. Assoc. Equip. **483**, 46 (2002).
39. Y. Hirata, M. Nakajima, Y. Nomura, et al., Phys. Rev. Lett. **110**, 187402 (2013).
40. G. Petrocelli, E. Pichini, F. Scudieri, et al., J. Opt. Soc. Am. B **10**, 918 (1993).
41. E. O. Kane, J. Phys. Chem. Solids **1**, 249 (1957).
42. C. Kittel, "Introduction to Solid State Physics," (Wiley, 2004).
43. A. G. Milnes and A. Y. Polyakov, Mater. Sci. Eng. B **18**, 237 (1993).
44. W. Nakwaski, Phys. B Phys. Condens. Matter **210**, 1 (1995).
45. G. A. Antcliffe and R. A. Stradling, Phys. Lett. **20**, 119 (1966).
46. M. A. Green, J. Appl. Phys. **67**, 2944 (1990).
47. M. Van Exter and D. Grischkowsky, Phys. Rev. B **41**, 12140 (1990).
48. M. Costato and L. Reggiani, Lett. Al Nuovo Cim. Ser. 1 **3**, 239 (1970).
49. W. Zawadzki and W. Szymańska, J. Phys. Chem. Solids **32**, 1151 (1971).
50. K. C. Rustagi, Phys. Rev. B **2**, 4053 (1970).
51. M. C. Hoffmann, J. Hebling, H. Y. Hwang, et al., Phys. Rev. B - Condens. Matter Mater. Phys. **79**, 3 (2009).
52. F. Meng, F. Walla, Q. Ul-Islam, et al., Phys. Rev. B **106**, 075203 (2022).

References with article titles

1. K. Makino, K. Kato, K. Takano, Y. Saito, J. Tominaga, T. Nakano, G. Isoyama, and M. Nakajima,"Significant Volume Expansion as a Precursor to Ablation and Micropattern Formation in Phase Change Material Induced by Intense Terahertz Pulses," Sci. Rep. **8**, 2914 (2018).
2. T. Kurihara, K. Hirota, H. Qiu, K. T. N. Phan, K. Kato, G. Isoyama, and M. Nakajima,"Reconfiguration of magnetic domain structures of ErFeO3 by intense terahertz free electron laser pulses," Sci. Rep. **10**, 7231 (2020).
3. N. Yoshikawa, T. Tamaya, and K. Tanaka,"High-harmonic generation in graphene enhanced by elliptically polarized light excitation," Science (80-.). **356**, 736 (2017)
4. R. Matsunaga, N. Tsuji, H. Fujita, A. Sugioka, K. Makise, Y. Uzawa, H. Terai, Z. Wang, H. Aoki, and R. Shimano,"Light-induced collective pseudospin precession resonating with Higgs mode in a superconductor," Science (80-.). **345**, 1145 (2014)
5. A. Iba, C. W. Domier, M. Ikeda, A. Mase, M. Nakajima, A.-V. Pham, and N. C. Luhmann,"Subdiffraction focusing with a long focal length using a terahertz-wave super-oscillatory lens," Opt. Lett. **46**, 4912 (2021).
6. M. A. Weiss, A. Herbst, J. Schlegel, T. Dannegger, M. Evers, A. Donges, M. Nakajima, A. Leitenstorfer, S. T. B. Goennenwein, U. Nowak, and T. Kurihara,"Discovery of ultrafast spontaneous spin switching in an antiferromagnet by femtosecond noise correlation spectroscopy," Nat. Commun. **14**, 7651 (2023).
7. J. Wang, W. Cai, W. Lu, S. Lu, E. Kano, V. C. Agulto, B. Sarkar, H. Watanabe, N. Ikarashi, T. Iwamoto, M. Nakajima, Y. Honda, and H. Amano,"Observation of 2D-magnesium-intercalated gallium nitride superlattices," Nature DOI:10.1038/s41586 (2024).
8. Y. W. Wang, S. Segawa, T. Shimizu, V. C. Agulto, V. K. Mag-usara, K. Kato, K. Miyamoto, T. Omatsu, K. Makino, J. Tominaga, G. Isoyama, M. Asakawa, and M. Nakajima,"Ablation phenomena by intense terahertz vortex beam," Appl. Phys. A Mater. Sci. Process. **128**, 836 (2022).
9. G. Fitzky, M. Nakajima, Y. Koike, A. Leitenstorfer, and T. Kurihara," Ultrafast Control of Magnetic Anisotropy by Resonant Excitation of 4f Electrons and Phonons in Sm0.7Er0.3FeO3," Phys. Rev. Lett. **127**, 107401 (2021).
10. D. Li, Y. Wang, M. Nakajima, M. Tani, M. Hashida, M. R. Asakawa, Y. Wei, and S. Miyamoto,"Coherent radiation at the fundamental frequency by a Smith-Purcell free-electron laser with dielectric substrate," Appl. Phys. Lett. **110**, 151108 (2017).
11. D. Li, M. Nakajima, M. Tani, J. Yang, H. Kitahara, M. Hashida, M. Asakawa, W. Liu, Y. Wei, and Z. Yang,"Terahertz Radiation from Combined Metallic Slit Arrays," Sci. Rep. **9**, 6804 (2019).
12. V. C. Agulto, T. Iwamoto, H. Kitahara, K. Toya, V. K. Mag-usara, M. Imanishi, Y. Mori, M. Yoshimura, and M. Nakajima,"Terahertz time-domain ellipsometry with high precision for the evaluation of GaN crystals with carrier densities up to 1020 cm−3," Sci. Rep. **11**, 18129 (2021).
13. V. C. Agulto, K. Toya, T. N. K. Phan, V. K. Mag-Usara, J. Li, M. J. F. Empizo, T. Iwamoto, K. Goto, H. Murakami, Y. Kumagai, N. Sarukura, M. Yoshimura, and M. Nakajima,"Anisotropic complex refractive index of β-Ga2O3 bulk and epilayer evaluated by terahertz time-domain spectroscopy," Appl. Phys. Lett. **118**, 42101 (2021).
14. M. Ota, K. Kan, S. Komada, Y. Wang, V. C. Agulto, V. K. Mag-usara, Y. Arikawa, M. R. Asakawa, Y. Sakawa, T. Matsui, and M. Nakajima,"Ultrafast visualization of an electric field under the Lorentz transformation," Nat. Phys. **18**, 1436 (2022).
15. M. Nagai, S. Aono, M. Ashida, K. Kawase, A. Irizawa, and G. Isoyama,"Luminescence induced by electrons outside zinc oxide nanoparticles driven by intense terahertz pulse trains," New J. Phys. **19**, 053017 (2017).
16. G. Ramian,"The new UCSB free-electron lasers," Nucl. Instruments Methods Phys. Res. Sect. A Accel. Spectrometers, Detect. Assoc. Equip. **318**, 225 (1992).
17. D. Oepts, A. F. G. van der Meer, and P. W. van Amersfoort,"The Free-Electron-Laser user facility FELIX," Infrared Phys. Technol. **36**, 297 (1995).
18. Y. U. Jeong, B. C. Lee, S. K. Kim, S. O. Cho, B. H. Cha, J. Lee, G. M. Kazakevitch, P. D. Vobly, N. G. Gavrilov, V. V Kubarev, and G. N. Kulipanov,"First lasing of the KAERI compact far-infrared free-electron laser driven by a magnetron-based microtron," Nucl. Instruments Methods Phys. Res. Sect. A Accel. Spectrometers, Detect. Assoc. Equip. **475**, 47 (2001).
19. K. Kawase, R. Kato, A. Irizawa, M. Fujimoto, S. Kashiwagi, S. Yamamoto, F. Kamitsukasa, H. Osumi, M. Yaguchi, A. Tokuchi, S. Suemine, and G. Isoyama,"The high-power operation of a terahertz free-electron laser based on a normal conducting RF linac using beam conditioning," Nucl. Instruments Methods Phys. Res. Sect. A Accel. Spectrometers, Detect. Assoc. Equip. **726**, 96 (2013).
20. M. R. Siegrist, F. Keilmann, C. Nieswand, and M. Urban,"Far-infrared wave generation by frequency tripling," Infrared Phys. Technol. **36**, 407 (1995).
21. K. J. Tielrooij, A. Principi, D. S. Reig, A. Block, S. Varghese, S. Schreyeck, K. Brunner, G. Karczewski, I. Ilyakov, O. Ponomaryov, T. V. A. G. de Oliveira, M. Chen, J. C. Deinert, C. G. Carbonell, S. O. Valenzuela, L. W. Molenkamp, T. Kiessling, G. V. Astakhov, and S. Kovalev,"Milliwatt terahertz harmonic generation from topological insulator metamaterials," Light Sci. Appl. **11**, 315 (2022).
22. H. A. Hafez, S. Kovalev, J. C. Deinert, Z. Mics, B. Green, N. Awari, M. Chen, S. Germanskiy, U. Lehnert, J. Teichert, Z. Wang, K. J. Tielrooij, Z. Liu, Z. Chen, A. Narita, K. Müllen, M. Bonn, M. Gensch, and D. Turchinovich,"Extremely efficient terahertz high-harmonic generation in graphene by hot Dirac fermions," Nature **561**, 507 (2018).
23. T. A. Uaman Svetikova, T. V. A. G. de Oliveira, A. Pashkin, A. Ponomaryov, C. Berger, L. Fürst, F. B. Bayer, E. G. Novik, H. Buhmann, L. W. Molenkamp, M. Helm, T. Kiessling, S. Winnerl, S. Kovalev, and G. V Astakhov,"Giant THz Nonlinearity in Topological and Trivial HgTe-Based Heterostructures," ACS Photonics **10**, 3708 (2023).
24. F. Meng, M. D. Thomson, Q. Ul-Islam, B. Klug, A. Pashkin, H. Schneider, and H. G. Roskos,"Intracavity third-harmonic generation in Si:B pumped by intense terahertz pulses," Phys. Rev. B **102**, 075205 (2020).
25. T. N. K. Phan, T. Shimizu, Y. W. Wang, K. Kato, V. C. Agulto, G. Isoyama, S. Fujioka, and M. Nakajima,"Third harmonic generation due to free carrier in InSb using a terahertz free electron laser," Opt. Lett. **49**, 1073 (2024).
26. P. A. Wolff and G. A. Pearson,"Theory of Optical Mixing by Mobile Carriers in Semiconductors," Phys. Rev. Lett. **17**, 1015 (1966).
27. P. Kaw,"Optical mixing by mobile carriers in semiconductors," Phys. Rev. Lett. **21**, 539 (1968).
28. C. C. Wang and N. W. Ressler,"Nonlinear Optical Effects of Conduction Electrons in Semiconductors," Phys. Rev. **188**, 1291 (1969).
29. K. C. Rustagi and S. S. Jha,"Effect of scattering on optical nonlinearities due to carriers in semiconductors," Phys. Lett. A **30**, 518 (1969).
30. R. W. Boyd,"Nonlinear Optics," Third Edit (Academic Press, 2008).
31. F. Meng, F. Walla, S. Kovalev, J.-C. Deinert, I. Ilyakov, M. Chen, A. Ponomaryov, S. G. Pavlov, H.-W. Hübers, N. V. Abrosimov, C. Jungemann, H. G. Roskos, and M. D. Thomson,"Higher-harmonic generation in boron-doped silicon from band carriers and bound-dopant photoionization," Phys. Rev. Res. **5**, 043141 (2023).
32. W. K. Burns and N. Bloembergen,"Third-harmonic generation in absorbing media of cubic or isotropic symmetry," Phys. Rev. B **4**, 3437 (1971).
33. D. J. Moss, H. M. van Driel, and J. E. Sipe,"Dispersion in the anisotropy of optical third-harmonic generation in silicon," Opt. Lett. **14**, 57 (1989).
34. P. A. Shaw, E. Forsyth, F. Haseeb, S. Yang, M. Bradley, and M. Klausen,"Two-Photon Absorption: An Open Door to the NIR-II Biological Window?," Front. Chem. **10**, 921354 (2022).
35. K. D. Belfield, S. Yao, and M. V. Bondar,"Two-photon absorbing photonic materials: From fundamentals to applications," Adv. Polym. Sci. **213**, 97 (2008).
36. K. Kawase, M. Nagai, K. Furukawa, M. Fujimoto, R. Kato, Y. Honda, and G. Isoyama,"Extremely high-intensity operation of a THz free-electron laser using an electron beam with a higher bunch charge," Nucl. Instruments Methods Phys. Res. Sect. A Accel. Spectrometers, Detect. Assoc. Equip. **960**, 163582 (2020).
37. G. Isoyama,"Development of a Free-Electron Laser in the Terahertz Region," JAS4QoL **6**, 2 (2020).
38. R. Kato, R. A. V Kumar, M. Kuwahara, M. Fujimoto, Y. Nakamura, T. Igo,

T. Konishi, S. Isaka, S. Mitani, S. Okuda, S. Suemine, and G. Isoyama,“Higher harmonic generation observed in SASE in the far-infrared region,” Nucl. Instruments Methods Phys. Res. Sect. A Accel. Spectrometers, Detect. Assoc. Equip. **483**, 46 (2002).

39. Y. Hirata, M. Nakajima, Y. Nomura, H. Tajima, Y. Matsushita, K. Asoh, Y. Kiuchi, A. G. Eguiluz, R. Arita, T. Suemoto, and K. Ohgushi,“Mechanism of enhanced optical second-harmonic generation in the conducting pyrochlore-type Pb2Ir2O7-x oxide compound,” Phys. Rev. Lett. **110**, 187402 (2013).
40. G. Petrocelli, E. Pichini, F. Scudieri, and S. Martellucci,“Anisotropic effects in the third-harmonic-generation process in cubic crystals,” J. Opt. Soc. Am. B **10**, 918 (1993).
41. E. O. Kane,“Band structure of indium antimonide,” J. Phys. Chem. Solids **1**, 249 (1957).
42. C. Kittel,“Introduction to Solid State Physics,” (Wiley, 2004).
43. A. G. Milnes and A. Y. Polyakov,“Indium arsenide: a semiconductor for high speed and electro-optical devices,” Mater. Sci. Eng. B **18**, 237 (1993).
44. W. Nakwaski,“Effective masses of electrons and heavy holes in GaAs, InAs, A1As and their ternary compounds,” Phys. B Phys. Condens. Matter **210**, 1 (1995).
45. G. A. Antcliffe and R. A. Stradling,“De Haas-Shubnikov effect in In Sb with high electron concentrations,” Phys. Lett. **20**, 119 (1966).
46. M. A. Green,“Intrinsic concentration, effective densities of states, and effective mass in silicon,” J. Appl. Phys. **67**, 2944 (1990).
47. M. Van Exter and D. Grischkowsky,“Carrier dynamics of electrons and holes in moderately doped silicon,” Phys. Rev. B **41**, 12140 (1990).
48. M. Costato and L. Reggiani,“Temperature-dependence of the combined effective mass of holes in silicon,” Lett. Al Nuovo Cim. Ser. 1 **3**, 239 (1970).
49. W. Zawadzki and W. Szymańska,“Electron scattering and transport phenomena in n-InSb,” J. Phys. Chem. Solids **32**, 1151 (1971).
50. K. C. Rustagi,“Effect of carrier scattering on nonlinear optical susceptibility due to mobile carriers in InSb, InAs, and GaAs,” Phys. Rev. B **2**, 4053 (1970).
51. M. C. Hoffmann, J. Hebling, H. Y. Hwang, K. Lo Yeh, and K. A. Nelson,“Impact ionization in InSb probed by terahertz pump-terahertz probe spectroscopy,” Phys. Rev. B - Condens. Matter Mater. Phys. **79**, 3 (2009).
52. F. Meng, F. Walla, Q. Ul-Islam, A. Pashkin, H. Schneider, C. Jungemann, M. D. Thomson, and H. G. Roskos,“Importance of valence-band anharmonicity and carrier distribution for third- and fifth-harmonic generation in Si:B pumped with intense terahertz pulses,” Phys. Rev. B **106**, 075203 (2022).